Supporting Information

Gil-da-Costa et al. 10.1073/pnas.1312264110

SI Materials and Methods

Stimuli Presentation. There are a variety of possible oddball paradigms manipulating different parameters such as frequency, intensity, or duration. In this study, we use intensity oddballs as this manipulation has been widely used and (critically for our experiments) has been shown to be effective in nonhuman primates (NHPs) (1).

NHPs were trained to maintain central fixation through positive reinforcement using standard techniques (2). The target appeared before the beginning of auditory stimulus presentation and remained visible for the entire duration of the recording session (i.e., 18 min). Precise eye-position control was not a requirement for this study because we were studying responses to auditory stimuli. The fixation target was merely an aid to help minimize ocular movement, and fixation was not quantified.

EEG Data Collection/Recordings. Collection of NHP EEG data required several additional steps, including:

i) Stabilizing NHP head position: rigid head fixation was required, so we designed an MR-compatible head post for surgical implantation on the dorsal cranium.

ii) NHP EEG setup: a customized EEG cap for macaque subjects was designed and developed in our laboratory. Using the same stretchable materials used for humans, we modified the human round cap to a two-panel design that allowed for a snug fit over the monkey scalp. This NHP cap (Fig. S1*B*) has 22 channels and an electrode density (electrodes 1 cm apart) identical to the human 64-channel cap (Fig. S1*A*). The cap was designed to fit the Ag/AgCl electrodes from the BrainAmp MR system used in human subjects.

iii) NHP EEG restraining chair: a custom-built MR-compatible chair (Fig. S1*B*) was designed in collaboration with Applied Prototypes using MR-compatible materials. NHPs were restrained inside the chair in a sphinx-like position with head protruding, stabilized, and facing forward.

iv) Three-dimensional scalp reconstruction with electrode positions: using the Polhemus Fastrak system, we created a 3D reconstruction of each animal's scalp with the exact position of each electrode pinpointed. This allowed us to create topographic maps of voltage distribution for acquired EEG datasets.

Animals were habituated to the EEG-acquisition procedures and trained on visual fixation using positive reinforcement before recordings.

EEG Data Analysis. The same analyses were applied to data from humans and monkeys. The analysis procedure began with rereferencing the datasets from their original recording references (human, Fcz; rhesus macaque, Pz) to posterior occipital channels, so as to provide a comparable reference between species (human: average of channels Oz, O1, O2, PO7, PO8, P7, and P8; rhesus macaque: average of channels Oz, O1, O2, P3, and P4). This was followed by band-pass filtering (low cutoff, 0.1 Hz; high cutoff, 50 Hz) and by down-sampling from 1,000 to 250 Hz based on spline interpolation. To avoid analysis artifacts stemming from differences in the number of standard ($n = 1{,}200$) and deviant ($n = 300$) trials, we first segmented the datasets relative to the deviant markers position (start, −1,000 ms; end, 600 ms), so that it would include all deviant trials ($n = 300$) and only the standard trials ($n = 300$) immediately preceding the deviants. We then segmented the resulting epochs relative to either the deviant or the standard marker positions (start, −200 ms; end, 600 ms) identifying the relevant deviant and standard epochs. For both standard and deviant epochs we applied: a baseline correction (start, −200 ms; end, 0 ms), a multiple features artifact rejection tool applied to all channels (i.e., maximal allowed voltage step, 50 μV/ms; maximal allowed difference of values in intervals, 200 μV; lowest allowed activity in intervals, 0.5 μV). The event-related potential (ERP) (average) was then calculated for each channel and condition (high-standard, low-standard, high-deviant, and low-deviant). Difference waves (deviant minus standard) were calculated for both conditions (i.e., low-deviant minus low-standard and high-deviant minus high-standard), and, subsequently, the low and high difference waves were averaged to yield the mismatch negativity (MMN) component, and the low and high responses to deviants were averaged to yield the P3a component.

Ketamine and Saline (Vehicle) Injections. The animals showed no overt behavioral signs of the ketamine effects under this testing paradigm (i.e., no signs of drowsiness and no observable differential behavior between the ketamine and saline injection conditions). It is important to note, however, that we used a passive listening oddball paradigm. Based upon previous reports (3), we would expect that behavioral changes should be observable using an appropriate behavioral paradigm, in association with the reported ketamine-modulated reductions of MMN and P3a.

Source Analysis. The estimation of the intracranial generators of each ERP component (MMN and P3a) was performed using low-resolution brain electromagnetic tomography (LORETA), an inverse-solution method (4, 5). We applied this source localization method to our human and NHP datasets using the Cartool 3.43 software. The LORETA inverse solution was estimated across two time intervals per species: human (56–188 ms and 208–256 ms) and NHP (48–120 ms and 104–248 ms) corresponding to the MMN and P3a components, respectively. The intracranial current distributions were computed in a grid of 5,000 solution points for human and 5,000 solution points for NHPs, regularly distributed within the gray matter of the cerebral cortex and limbic structures of the average brain provided by the Montreal Neurological Institute (MNI 152) for the human and of magnetic resonance imaging scans of our animals for the NHP data. No a priori assumptions were made for the location and number of active sources.

1. Javitt DC, Schroeder CE, Steinschneider M, Arezzo JC, Vaughan HG, Jr. (1992) Demonstration of mismatch negativity in the monkey. *Electroencephalogr Clin Neurophysiol* 83(1): 87–90.
2. Huang X, Albright TD, Stoner GR (2008) Stimulus dependency and mechanisms of surround modulation in cortical area MT. *J Neurosci* 28(51):13889–13906.
3. Leopold DA, Plettenberg HK, Logothetis NK (2002) Visual processing in the ketamine-anesthetized monkey. Optokinetic and blood oxygenation level-dependent responses. *Exp Brain Res* 143(3):359–372.
4. Michel CM, et al. (2004) EEG source imaging. *Clin Neurophysiol* 115(10):2195–2222.
5. Pascual-Marqui RD, Michel CM, Lehmann D (1994) Low resolution electromagnetic tomography: A new method for localizing electrical activity in the brain. *Int J Psychophysiol* 18(1):49–65.

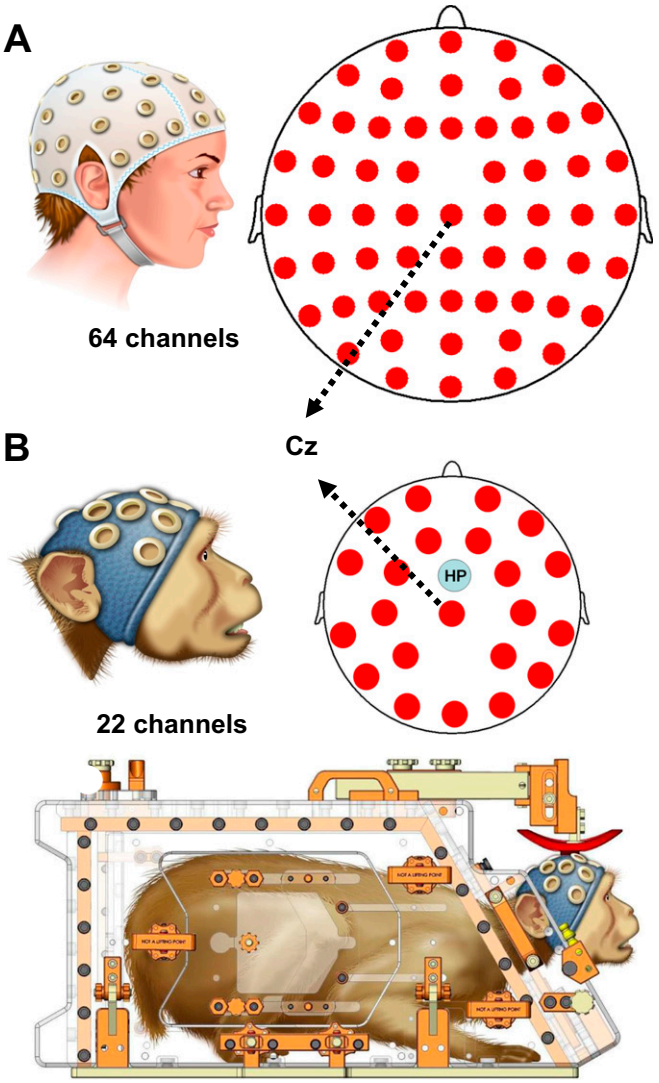

Fig. S1. Illustration of the EEG caps for both species and of the NHP chair. (*A*) Schematic of the 64-channel human EEG cap BrainCap MR (Brain Products) electrode locations (red). (*B*) Schematic of the customized 22-channel NHP EEG cap electrode locations (red) and head post (HP) (blue). (*B*, *Lower*) An illustration of the custom-built NHP chair, designed in collaboration with Applied Prototypes, in which the subject sits in a sphinx-like position. The chair was designed to be MR-compatible. The location of the Cz electrode is marked in both the human and the NHP cap schematics.

Table S1. MMN statistical analysis

Comparison	df	*N*	*F*	*P*
Human				
Standard vs. deviant (no injection)	1	1,264	97.127	<0.001
NHP				
Standard vs. deviant (no injection)	1	411	11.172	<0.001
Ketamine (NMDAR antagonist) vs. saline (vehicle)	1	292	43.982	<0.001
Ketamine (NMDAR antagonist) vs. 5 h postketamine	1	405	58.481	<0.001
5 h postketamine vs. saline (vehicle)	1	292	0.15383	>0.05

NMDAR, NMDA receptor.

Table S2. MMN variance

Physiological condition	Stimulus condition	Stimulus type	SD
Human			
No injection	Standard	High	7.898857
No injection	Deviant	High	7.971153
No injection	Standard	Low	8.363680
No injection	Deviant	Low	8.419159
NHP			
No injection	Standard	High	12.25324
No injection	Deviant	High	9.98598
No injection	Standard	Low	8.38422
No injection	Deviant	Low	10.51076
Ketamine (NMDAR antagonist)	Standard	High	9.61579
Ketamine (NMDAR antagonist)	Deviant	High	8.67129
Ketamine (NMDAR antagonist)	Standard	Low	7.56571
Ketamine (NMDAR antagonist)	Deviant	Low	9.71045
Saline (vehicle)	Standard	High	11.29175
Saline (vehicle)	Deviant	High	10.79641
Saline (vehicle)	Standard	Low	9.79885
Saline (vehicle)	Deviant	Low	13.21218
5 h post ketamine	Standard	High	10.57871
5 h post ketamine	Deviant	High	11.16715
5 h post ketamine	Standard	Low	10.08445
5 h post ketamine	Deviant	Low	11.36654

Table S3. P3 statistical analysis

Comparison	df	*N*	*F*	*P*	*t*
Human					
Deviant vs. zero (no injection)	1,281	1,282	NA	<0.01	37.52876
NHP					
Deviant vs. zero (no injection)	440	441	NA	<0.01	31.89494
Ketamine (NMDAR antagonist) vs. Saline (vehicle)	1	303	27.733	<0.001	NA
Ketamine (NMDAR antagonist) vs. 5 h post ketamine	1	413	44.336	<0.001	NA
5 h postketamine vs. saline (vehicle)	1	303	0.06226	>0.05	NA

NA, not available.

Table S4. P3 variance

Physiological condition	Stimulus condition	Stimulus type	SD
Human			
No injection	Deviant	High	9.216284
No injection	Deviant	Low	9.024022
NHP			
No injection	Deviant	High	9.517968
No injection	Deviant	Low	12.06867
Ketamine (NMDAR antagonist)	Deviant	High	9.17057
Ketamine (NMDAR antagonist)	Deviant	Low	10.38864
Saline (vehicle)	Deviant	High	11.05877
Saline (vehicle)	Deviant	Low	13.35940
5 h postketamine	Deviant	High	10.16603
5 h postketamine	Deviant	Low	10.79196